Polish Polar Research
DOI:10.24425/ppr.2026.8077

THIS IS AN ACCEPTED ARTICLE.
This article has been accepted for publication in a future issue of *PPRes*, but has not been fully edited. Content may change prior to final publication.

Atmospheric radionuclides accumulation in supraglacial sediments and mosses on two Arctic glaciers in Svalbard

Katarzyna KOŁTONIK[1]* ORCID-0000-0002-7549-1567, Krzysztof ZAWIERUCHA[2,3] ORCID-0000-0002-0754-1411, Jakub BUDA[2] ORCID-0000-0002-4584-5897, Dariusz SALA[1] ORCID-0000-0003-1723-0008, Kamil WOJCIECHOWSKI[1] ORCID-0009-0000-4219-8498, Krzysztof SAMOLEJ[4] ORCID-0000-0002-0867-7556, Mariusz WIERZGOŃ[5] ORCID-0000-0002-4809-2202, Anna CWANEK[1] ORCID-0000-0002-2574-807X, Michał BONCZYK[4] ORCID-0000-0002-9355-2271 and Edyta ŁOKAS[1] ORCID-0000-0001-9996-6523

[1] *Institute of Nuclear Physics, Polish Academy of Sciences, Radzikowskiego 152, 31-342 Kraków, Poland*
[2] *Department of Animal Taxonomy and Ecology, Adam Mickiewicz University, Uniwersytetu Poznańskiego 6, 61-614 Poznań, Poland*
[3] *Institute of Biochemistry and Biophysics, Polish Academy of Sciences, Pawińskiego 5a, 02-106 Warszawa, Poland*
[4] *Silesian Centre for Environmental Radioactivity, Central Mining Institute - National Research Institute (GIG-PIB), Plac Gwarków 1, 40-166 Katowice, Poland*
[5] *Faculty of Natural Sciences, University of Silesia in Katowice, Jagiellońska 28, 40-032 Katowice, Poland*

***corresponding author:** katarzyna.koltonik@ifj.edu.pl

Received 1 June 2026 **Accepted** 29 October 2026

Running title: Atmospheric radionuclides in supraglacial sediments and mosses

Abstract: Radionuclide accumulation in glacial environments is of increasing concern due to its potential ecological implications associated with retreat of glaciers worldwide. Identifying suitable matrices for monitoring radionuclides in glacial environments is therefore important for assessing their environmental availability and potential downstream transport. This study aimed to assess the occurrence of artificial (^{137}Cs, $^{239+240}$Pu) and natural (^{210}Pb) radionuclides in glacier mice and cryoconite (supraglacial sediments) from Svalbard. Samples were collected from two glaciers (Longyearbreen and

This article has been accepted for publication in a future issue of PPRes, but has not been fully edited. Content may change prior to final publication.

Polish Polar Research - Accepted Article

Foxfonna), with glacier mice present at one site. Additionally, we compared our results with activity concentration from other studies on radionuclides in cryoconite and plants on Svalbard, as well as a few available studies on glacier mice in general. Investigated radionuclides were found in both matrices, while cryoconite generally exhibited higher activity concentrations than glacier mice. The $^{240}Pu/^{239}Pu$ atomic ratios indicate that global fallout is the primary source of these isotopes. Glacier mice were created by two species of moss, *Sanionia nivalis* and *Hygrohypnella polaris*. Radionuclide concentrations in the glacier mice and cryoconite in Central Spitsbergen are lower than those previously reported for cryoconite in the Arctic. We corroborate that cryoconite is a more robust matrix for radionuclide monitoring and demonstrate that glacier mice have potential as complementary biomonitors for studies on radionuclide availability in Arctic glacial environments. The use of glacier mice as biomonitors may provide new insights into the transport, deposition, and accumulation of contaminants at glacier forefields.

Keywords: Arctic, glacier mice, cryoconite, radioisotopes, global fallout.

Introduction

The Svalbard archipelago, located in the European Arctic, is experiencing rapid climate warming, with reported rates up to seven times higher than those observed in other regions (ACIA 2005; Serreze and Barry 2011; Schuler *et al.* 2025). Despite its high-latitude location, Svalbard is witnessing relatively moderate conditions due to the influence of the North Atlantic Current, an extension of the Gulf Stream. Glaciers are a major component of Svalbard's landscapes and ecosystems, covering more than 50% of the archipelago's land area (Schuler *et al.* 2020). The largest island, Spitsbergen, serves as a natural laboratory for Arctic environmental studies owing to its natural mosaic landscapes, a network of scientific stations, and long-term monitoring of biotic and abiotic environments (Coulson 2013; Senger *et al.* 2025).

Svalbard is an important monitoring site for observing the real-time effects of global warming, anthropogenic impacts on ecosystems located far from industrialized areas, and the melting of different components of the cryosphere (Jania *et al.* 2015; Ignatiuk *et al.* 2022; Christiansen *et al.* 2024). In recent years, Svalbard has attracted increasing scientific attention in the context of radioactive contamination, owing to its relatively pristine environment and the high sensitivity of Arctic ecosystems to pollutants (Łokas *et al.* 2016), including also the potential for contamination associated with nuclear weapons testing in the Arctic.

Regional monitoring indicates low levels of radionuclide contamination in both marine and terrestrial environments (Gwynn *et al.* 2004; Łokas *et al.* 2013, 2017a, 2019). The

Polish Polar Research - Accepted Article

This article has been accepted for publication in a future issue of PPRes, but has not been fully edited. Content may change prior to final publication.

primary transport pathways include atmospheric circulation, marine currents, and sea ice (Zaborska 2017; Burakowska *et al.* 2021; Cwanek *et al.* 2026). Over the past decades, the occurrence and sources of radioactive contamination in Svalbard have been investigated across various environmental matrices (Saniewski *et al.* 2000; Dowdall *et al.* 2003; Gwynn *et al.* 2004; Chmiel *et al.* 2009; Kłos *et al.* 2017; Łokas *et al.* 2013, 2014, 2016, 2017a, 2017b, 2019; Cwanek *et al.* 2020). Artificial radionuclide deposition in the Svalbard region originates from multiple sources; however, the predominant sources of radionuclide contamination are global fallout from atmospheric nuclear weapons testing conducted between 1945 and 1980 (UNSCEAR 2000), as well as the disintegration of a satellite carrying the SNAP-9A radioisotope thermal generator in 1964 (Krey 1967). Additional, albeit smaller, contributions are attributable to the Chernobyl nuclear accident in 1986 (Gwynn *et al.* 2004; Cwanek *et al.* 2020) and the Fukushima Daiichi disaster in 2011 (Paatero *et al.* 2012). Furthermore, given Svalbard's geographic proximity to the nuclear test sites at Novaya Zemlya, where predominantly high-yield detonations were conducted (UNSCEAR 2000; García-Tenorio 2018), and Semipalatinsk, which was primarily used for low-yield nuclear tests (Wendel et al. 2013; García-Tenorio 2018), both sites are considered potential sources of radionuclides in the Svalbard environment.

The intensification of military activities, including missile testing and the expansion of strategic infrastructure, together with the planned deployment of small modular reactors (SMRs), may represent additional sources of radionuclide release to the environment in remote Arctic regions (Bouville 2020; Stocki 2026). Although these activities are subject to strict safety regulations, accidental emissions, operational discharges, and the remobilization of historically deposited radionuclides cannot be excluded. Recent findings from air filter samples collected in southwestern Spitsbergen revealed elevated levels of ^{241}Am, ^{237}Np, and ^{238}Pu, which could not be attributed to natural processes and may indicate recent radioactive emissions (Cwanek *et al.* 2026).

The isotopic composition of plutonium in air filters from Svalbard showed enrichment of ^{238}Pu relative to $^{239+240}$Pu, suggesting contributions from sources other than global fallout (Cwanek *et al.* 2026). The distribution of plutonium isotopes in the environment is influenced by both local resuspension and long-range atmospheric transport. Atmospheric trajectory simulations indicate that the primary transport pathways of radionuclide contaminants originate from northern Eurasia (Cwanek *et al.* 2026).

The isotopic composition of plutonium provides an important tool for identifying contamination sources because different plutonium sources can exhibit distinct isotopic signatures. In particular, the ^{240}Pu/^{239}Pu atomic ratio is widely used as a source tracer because

Polish Polar Research - Accepted Article

This article has been accepted for publication in a future issue of PPRes, but has not been fully edited. Content may change prior to final publication.

global atmospheric fallout from nuclear weapons testing has a relatively well-characterized isotopic signature, whereas releases associated with specific nuclear activities or accidents may exhibit different ratios. Consequently, comparison of measured $^{240}Pu/^{239}Pu$ atomic ratios with characteristic values for global fallout can help distinguish the contribution of global fallout from potential regional or other sources of plutonium. In contrast, the $^{238}Pu/^{239+240}Pu$ activity ratio may be more sensitive to temporal changes associated with atmospheric transport, resuspension, and additional contamination sources (Salminen-Paatero *et al.* 2020). Therefore, the $^{240}Pu/^{239}Pu$ atomic ratio was determined as a more reliable tracer for identifying the origin of plutonium contamination.

Two types of supraglacial material, cryoconite and glacier mice, provide valuable opportunities to investigate the accumulation and distribution of fallout radionuclides in glacial environments. Cryoconite is a dark-colored, biogenic, often granular sediment occurring on glacier surfaces (Rozwalak *et al.* 2022). It consists mainly of mineral particles (70–95%) and organic matter (1–38%), which accumulate within cryoconite holes (Takeuchi *et al*. 2001; Cook *et al*. 2016; Rozwalak *et al.* 2022) or are dispersed across the ice surface (Baccolo *et al*. 2020). The dark colour of cryoconite reduces glacier surface albedo, thereby enhancing solar radiation absorption and accelerating surface melting processes (Baccolo *et al*. 2020). This process contributes to the formation of cryoconite holes, which are water-filled microhabitats on glacier surfaces recognized as biodiversity hotspots and important centres of biogeochemical activity (Cook *et al*. 2016; Buda *et al*. 2020).

Recently, glacier mice (bryophyte aggregations growing on the glacier surface) have been proposed as a valuable additional environmental matrix for tracking atmospheric contaminants in the glaciated regions (Kołtonik *et al.* 2024; Smith *et al.* 2024). The ability of bryophytes to accumulate atmospheric pollutants is well documented (Kołtonik *et al.* 2024). Therefore, comparing glacier mice with cryoconite may help to elucidate the role of glacier mice in the accumulation, retention, and cycling of inorganic pollutants within glacier ecosystems (Kołtonik *et al.* 2024). These structures have been shown to accumulate radionuclides on the ice surface and facilitate their transport to proglacial environments, playing an important role in the cycling of radioactive contaminants within developing proglacial ecosystems (Kołtonik *et al.* 2024). Contaminants persisting on ice surfaces may bioaccumulate and biomagnify within organisms living on glaciers, potentially altering their behavior and metabolic functions, as demonstrated in various groups of organisms (*e.g.*, Lencioni *et al.* 2023; Buda *et al.* 2024; Crosta *et al.* 2024).

Comparing glacier mice with cryoconite in the Arctic represents a further step towards understanding pollution in supraglacial environments. It is based on the fact that both

Polish Polar Research - Accepted Article

This article has been accepted for publication in a future issue of PPRes, but has not been fully edited. Content may change prior to final publication.

represent natural biomonitors of atmospherically transported particles within glacier ecosystems, although they differ in their biological composition, structure, and mechanisms of contaminant retention (*e.g.*, Hotaling *et al.* 2020). Glacier mice are composed primarily of mosses, which are well known for their ability to accumulate radionuclides and trace elements directly from atmospheric deposition. Mosses have long been used as biomonitors of environmental contamination because they efficiently retain airborne particles on their surfaces and incorporate deposited contaminants into their tissues (Harmens *et al.* 2015). Furthermore, the dense structure of glacier mice promotes the trapping of mineral dust and atmospheric aerosols, which frequently act as carriers of radionuclides. Their relatively long residence time on glacier surfaces (Hotaling *et al.* 2020) also enables the continuous accumulation of contaminants over extended periods. As rare components of cryospheric ecosystems, glacier mice and other bryophytes associated with glacial ecosystems warrant investigation, particularly given their potential for disappearance due to glacier retreat (Uetake *et al.* 2002; Zawierucha *et al.* 2026). Although the Svalbard archipelago is a natural laboratory for environmental studies, glacier mice in this area have not been studied in the context of pollution.

The primary objective of this study was to determine, for the first time, the activity concentrations of ^{137}Cs, $^{239+240}$Pu, and ^{210}Pb in glacier mice, and to compare their accumulation with that observed in cryoconite collected from Longyearbreen and Foxfonna in Spitsbergen. Additionally, we analyzed the ^{240}Pu/^{239}Pu atomic ratio to assess whether the plutonium contamination was consistent with global atmospheric fallout or indicated contributions from other sources. By comparing glacier mice with cryoconite, we aimed to evaluate the potential of glacier mice as a complementary biological matrix for monitoring radionuclide contamination in Arctic glaciers (Svalbard) and subarctic glaciers (Iceland and Norway).

Study area

The Svalbard archipelago is part of Norway and is located in the Arctic Ocean, with the Greenland Sea to the west, the Norwegian Sea to the south, and the Barents Sea to the east. During the 1981–2010 reference period, mean seasonal air temperatures at Svalbard Airport ranged from −11.7°C in winter to 5.2°C in summer. Long-term observations from the same station indicate a mean annual air temperature of −4.5°C for the period of 1979–2014, with February being the coldest month (mean temperature of −13.9°C) and July being the warmest month (6.4°C) (Osuch and Wawrzyniak 2017; Wawrzyniak and Osuch 2020). Over the past three decades, average temperatures have risen by approximately 4°C, at a rate six times the global average during the 21st century. The mean annual precipitation at Svalbard Airport is

Polish Polar Research - Accepted Article

This article has been accepted for publication in a future issue of PPRes, but has not been fully edited. Content may change prior to final publication.

191 mm, whereas at Ny-Ålesund it is higher, reaching 427 mm (Førland *et al.* 2011). Long-term observational records indicate an increasing trend, and model projections suggest a further rise in precipitation towards the end of the 21st century (Førland *et al.* 2011).

In this study, we focus on the two glaciers in central Svalbard: the valley glacier Longyearbreen and the ice cap Foxfonna. Longyearbreen (78°10′ N, 15°30′ E) is situated in Adventfjorden, a branch of Isfjorden, within the central part of Spitsbergen (Svalbard). The glacier has a northeast-facing orientation and covered approximately 2.5 km^2 in 2010 (Langford *et al.* 2014). Its elevation ranges from ~250 m to ~1000 m a.s.l. (Langford *et al.* 2014). The glacier's catchment is underlain by coal-bearing shales, siltstones, and sandstones (Yde *et al.* 2008). Foxfonna (78.14° N, 16.11° E) is a 6 km^2 ice cap with a north-facing outlet glacier located in central Spitsbergen (Rassner *et al.* 2024). The glacier extends from approximately 380 to 810 m a.s.l. (Christiansen *et al.* 2005). The surrounding bedrock is primarily composed of sandstone, siltstone, and shale (Major and Nagy 1972).

Sampling

A total of 45 samples representing three environmental matrices were collected during fieldwork conducted in mid-July 2023 (Table S1). These included 15 glacier mice collected from glacier surfaces, 25 cryoconite samples collected from cryoconite holes, and five bryophyte samples collected from the lateral moraine. The three matrices were selected to compare radionuclide accumulation in non-glacial (glacier mice and terrestrial bryophytes) and glacial (cryoconite) environments.

Mosses (glacier mice from the glacier surface and mosses from moraine) were sampled exclusively at Foxfonna, as glacier mice were not observed on Longyearbreen during the 2023 summer field season. Cryoconite was collected from both Foxfonna and Longyearbreen to enable comparison between glaciers. Glacier mice were collected manually and placed in polyethylene zip-lock bags, whereas cryoconite was sampled from cryoconite holes using disposable Pasteur pipettes and transferred into polypropylene tubes to minimize cross-contamination. Detailed information on individual samples is provided in Table S1, and sampling locations are shown in Figs. 1 and 2.

Methods

Bryophyte identification

Bryophytes were examined using standard methods and identified to the species level by using the key by Hedenäs *et al.* (2014). Nomenclature for bryophytes was adopted from Lönnell *et al.* (2025). The specimens are stored in the Bryophyte Herbarium of the National

Polish Polar Research Accepted Article

This article has been accepted for publication in a future issue of PPRes, but has not been fully edited. Content may change prior to final publication.

Biodiversity Collection at W. Szafer Institute of Botany, Polish Academy of Sciences (KRAM).

Gamma spectrometry

The samples were dried at 100°C before gamma spectrometry analysis. Radioactive analyses were conducted at the ISO/IEC 17025:2018-2 accredited facility at the Central Mining Institute – National Research Institute (Poland). The measurements were performed according to the internal protocol SCR/ZLGIG/2-004, accredited by the Polish Center for Accreditation (AB 005). Gamma counting was conducted with a high-purity germanium detector (HPGe), cooled by liquid nitrogen (LN2). A planar broad-energy detector (BEGe™) with a relative efficiency of 50% (BE5030, Canberra) was used. The detector performance, expressed as full width at half maximum (FWHM) for the 609 keV line of ^{214}Bi, was 1.35 keV.

The energy and efficiency calibration was performed using a multi-gamma source containing isotopes emitting gamma rays over a wide energy range (46–2000 keV). This source was prepared using reference materials (RM) containing natural radionuclides – RGU-1, RGTh-1, and RGK-1 provided by the International Atomic Energy Agency (IAEA). Calibration relationships were established using Canberra Genie 2000 software. The reported measurement uncertainties represent the total uncertainty. The activity concentrations of ^{210}Pb and ^{137}Cs were determined using the following energy lines: ^{210}Pb (46.5 keV) and ^{137}Cs (662 keV).

Quality control analyses were performed using samples from IAEA-certified reference materials: a moss-soil sample (IAEA-447) and a soil sample (IAEA-444). According to the producer, IAEA-447 consists of decomposition products of moss, rock minerals from erosion/weathering processes, and any washed-in soil, while IAEA-444 is a soil spiked with gamma-emitting radionuclides (Table S2).

Mass spectrometry

Following gamma spectrometry, the samples were dried at 100°C, burned at 600°C, and subjected to radiochemical preparation. A ^{242}Pu radioactive tracer (Standard Reference Material 4334J, NIST) was added, after which the samples were dissolved using a mixture of HF, HNO_3, HCl, and boric acid. Plutonium was stabilized in the +IV oxidation state using $NaNO_2$ and subsequently separated from 8 M HNO_3 by ion-exchange chromatography with AmberChrom 1 × 8 resin (Sigma-Aldrich).

The samples were then evaporated to dryness, stabilized in the +IV oxidation state, and finally 3 M HNO_3 solution was prepared. The solution was loaded onto columns containing TEVA resin (Triskem International, France). The plutonium fraction was eluted using a mixture of 0.1 M HCl and 0.1 M HF. The plutonium fraction was then converted and

Polish Polar Research - Accepted Article

This article has been accepted for publication in a future issue of PPRes, but has not been fully edited. Content may change prior to final publication.

dissolved in a 2% HNO_3/0.25% HF mixture. Both the concentrations of ^{239}Pu and ^{240}Pu, as well as the $^{240}Pu/^{239}Pu$ atomic ratio, were determined using an Agilent 8900#100 ICP-QQQ instrument (Agilent Technologies, USA).

To enhance sensitivity, an external desolvating nebulizer (APEX, ESI, USA) was coupled to the mass spectrometer. Plutonium isotopes were measured in mass shift mode (+32 amu) by introducing O_2 gas into the collision/reaction cell (CRC) to minimize polyatomic interferences. An external mass bias correction was performed using the exponential law (Taylor *et al*. 2001), based on measurements of the IRMM-290 standard certified for the $^{239}Pu/^{242}Pu$ atomic ratio. Data quality was assessed using the IAEA-447 moss–soil certified reference material (Table S3).

Statistical analysis

Statistical analysis covered radioactivity concentrations and, due to the nature of the data, nonparametric tests were used to determine the statistical significance of differences between groups. Depending on the compared variable and available data, different approaches were used due to limitations in sample size.

Analysis of differences in ^{137}Cs activity concentration was limited, as only results from Foxfonna were available. In this case, differences were tested between cryoconite and glacier mice, as there were not enough bryophytes results to create a sample of an appropriate size. Differences in ^{137}Cs concentration between cryoconite and glacier mice on Foxfonna were tested using the U Mann-Whitney test.

Analysis of ^{210}Pb activity concentration comprised two steps, as a hierarchical analysis including two factors (glacier and sample type) was unfeasible due to differences in group sizes: Foxfonna glacier had all three sample type groups (cryoconite, bryophytes from lateral moraine, glacier mice), while Longyearbreen had only one group (cryoconite). Thus, the analysis was split into two steps: (*i*) analyzing differences in ^{210}Pb activity concentration in cryoconite between Longyearbreen and Foxfonna glacier using the U Mann-Whitney test, and (*ii*) analyzing differences between cryoconite, glacier mice and bryophytes samples from Foxfonna using the Kruskall-Wallis test.

For the same reasons, a similar analysis was conducted for $^{239+240}Pu$ activity concentrations: the U Mann-Whitney test for differences in $^{239+240}Pu$ activity concentrations between two glaciers, and the Kruskal-Wallis test for differences between cryoconite, glacier mice, and bryophyte samples from Foxfonna glacier. Finally, the differences in the $^{240}Pu/^{239}Pu$ atomic ratio between cryoconite and glacier mice samples from Foxfonna glacier were tested using the U Mann-Whitney test.

Polish Polar Research - Accepted Article

This article has been accepted for publication in a future issue of PPRes, but has not been fully edited. Content may change prior to final publication.

Results

Glacier mice

Two moss species were identified: *Sanionia nivalis* Hedenäs and *Hygrohypnella polaris* (Lindb.) Ignatov & Ignatova. In all but one of the analysed samples, glacier mice consisted exclusively of *S. nivalis*.

Radioactivity and atomic ratio of cryoconite

The radionuclide activity concentrations of ^{137}Cs, ^{210}Pb, and $^{239+240}$Pu, together with the ^{240}Pu/^{239}Pu atomic ratios measured in the collected samples are presented in Fig. 3 and Table S1. Cryoconite from Foxfonna generally exhibited higher ^{137}Cs and $^{239+240}$Pu activity concentrations, whereas cryoconite from Longyearbreen contained higher ^{210}Pb activity concentrations.

The overall activity concentrations of ^{210}Pb, ^{137}Cs and $^{239+240}$Pu varied between the Longyearbreen and Foxfonna. The median ^{137}Cs activity concentration in cryoconite from Foxfonna was 12 Bq kg^{-1} (interquartile range, IQR = 41.5, n = 12), with values ranging from 6 Bq kg^{-1} to 242 Bq kg^{-1}, while the majority of the samples from Longyearbreen were below the detection limit (see Table S1). Higher median ^{210}Pb activity concentration was found in cryoconite from Longyearbreen (1400 Bq kg^{-1}; IQR = 1140, n = 13), with values ranging from 1001 Bq kg^{-1} to 3270 Bq kg^{-1}, compared with samples from Foxfonna (801 Bq kg^{-1}; IQR = 356, n = 12), where values ranged from 190 Bq kg^{-1} to 1240 Bq kg^{-1}. Cryoconite from Longyearbreen and Foxfonna exhibited significantly different ^{210}Pb activity concentrations ($p = 0.0001$). Higher median values of $^{239+240}$Pu were observed in cryoconite samples collected from Foxfonna (0.23 Bq kg^{-1}; IQR = 1.10, n = 12), with values ranging from 0.10 Bq kg^{-1} to 4.36 Bq kg^{-1}, compared with samples from Longyearbreen (0.09 Bq kg^{-1}; IQR = 0.07, n = 13), where values ranged from 0.05 Bq kg^{-1} to 0.18 Bq kg^{-1}. Significant differences in $^{239+240}$Pu were observed between cryoconite samples from Longyearbreen and Foxfonna ($p = 0.0001$). The median ^{240}Pu/^{239}Pu atomic ratio was likewise determined in samples from Foxfonna, with a value of 0.171 (IQR = 0.018, n = 12). In contrast, the ^{240}Pu/^{239}Pu atomic ratio was determined in only a few samples from Longyearbreen with a value of 0.171 (IQR = 0.043, n = 3).

Radioactivity and atomic ratio of glacier mice and bryophytes collected from moraine

Activity concentrations of ^{137}Cs, ^{210}Pb, and $^{239+240}$Pu in glacier mice were generally comparable to those measured in bryophytes from the lateral moraine, although glacier mice tended to exhibit higher median activity concentrations of ^{210}Pb and $^{239+240}$Pu (Fig. 3; Table S1). Comparable median ^{137}Cs activity concentrations were observed in glacier mice (28 Bq kg^{-1};

Polish Polar Research - Accepted Article

This article has been accepted for publication in a future issue of PPRes, but has not been fully edited. Content may change prior to final publication.

IQR = 5, range = 19–58 Bq kg^{-1}, n = 14) and in bryophytes collected from the lateral moraine at Foxfonna (27 Bq kg^{-1}; IQR = 10, range = 21–35 Bq kg^{-1}, n = 4).

Although glacier mice and moraine bryophytes showed comparable ^{137}Cs activity concentrations, glacier mice differed significantly from cryoconite collected at Foxfonna (p = 0.031). For ^{210}Pb, median activity concentrations were higher in the glacier mice (1004 Bq kg^{-1}; IQR = 302, range = 614–1495 Bq kg^{-1}, n = 14) than in bryophytes on the lateral moraine (775 Bq kg^{-1}; IQR = 622, range = 181–1592 Bq kg^{-1}, n = 5). Furthermore, no significant differences in ^{210}Pb activity concentrations were observed among glacier mice, bryophytes and cryoconite samples from Foxfonna (p = 0.1536).

Bryophytes exhibited lower median activity concentrations of $^{239+240}Pu$ (0.39 Bq kg^{-1}, IQR = 1.23; range = 0.06–1.73 Bq kg^{-1}; n = 5) compared with glacier mice (0.79 Bq kg^{-1}; IQR = 0.18, range = 0.43–1.23 Bq kg^{-1}, n = 14). No significant differences in $^{239+240}Pu$ activity concentrations were found among glacier mice, bryophytes, and cryoconite from Foxfonna (p = 0.3180). The median $^{240}Pu/^{239}Pu$ atomic ratio was higher in bryophytes (0.175; IQR = 0.011, n = 4) than in glacier mice (0.169; IQR = 0.043, n = 14). No significant differences in $^{240}Pu/^{239}Pu$ atomic ratio were found among cryoconite and glacier mice from Foxfonna (p = 0.4557).

Discussion

Mosses on glacier surface and moraine

Glacier mice on Foxfonna Glacier represented mostly pillow-like structures (Fig. 2) and differed from those described in the literature as spherical structures from lower latitudes (Coulson and Midgley 2012; Zawierucha *et al.* 2026). Both confirmed moss species represent an Arctic-alpine distribution pattern, occurring in northern Europe, including Svalbard, as well as Asia and North America (Hedenäs 2014; Hedenäs *et al.* 2014; Jamieson 2014). In polar and high-mountain areas, these species grow in highly hydrated habitats near streams fed by glaciers and snowmelt, as well as in boulder fields and snow beds (Hedenäs 1989; Hedenäs *et al.* 2014).

The creation of glacier mice by *Sanionia nivalis* has not been reported previously. In contrast, *Hygrohypnella polaris*, identified in only a single sample, is a component regular to this microhabitat type in Svalbard (Belkina and Mavlyuduv 2011; Belkina and Vilnet 2015). The mosses on the glacier surface were different in shape from those called glacier mice and found on Iceland or in Norway (Coulson and Midgley 2012; Zawierucha *et al.* 2026).

Radionuclides and nuclear contamination sources in Central Spitsbergen Glaciers

Polish Polar Research - Accepted Article

This article has been accepted for publication in a future issue of PPRes, but has not been fully edited. Content may change prior to final publication.

This study provides evidence that glacier mice can accumulate ^{137}Cs, ^{210}Pb, and $^{239+240}$Pu and may serve as complementary biomonitors of radionuclide deposition in High Arctic glacier ecosystems. The measured activity concentrations of ^{137}Cs, ^{210}Pb, and $^{239+240}$Pu indicate that glacier mice integrate signals from atmospheric deposition and local redistribution processes occurring within glacier environments. To compare the radionuclide concentration in glacier mice, bryophytes and other components from glacial and non-glacial environments, we subsequently used reports by Gwynn *et al.* (2004), Łokas *et al.* (2016, 2019, 2024), Smith *et al.* (2024), and Kołtonik *et al.* (2024, 2025).

Radionuclide contamination levels in the investigated glacier mice, bryophytes, and cryoconite were generally lower than those previously reported for the Svalbard region (Fig. 4; Gwynn *et al.* 2004; Łokas *et al.* 2013, 2016, 2017a, 2019). Studies on Longyearbreen showed that cryoconite granules disintegrate on the glacier surface of small valley glaciers during extreme weather events (Zawierucha *et al.* 2019), likely resulting in lower ^{137}Cs and $^{239+240}$Pu activity concentrations due to dilution, whereas no such pattern was observed for ^{210}Pb.

The highest mean ^{137}Cs activity concentrations in this study were observed in cryoconite, whereas glacier mice and bryophytes exhibited lower values (Fig. 4). ^{137}Cs on Svalbard comes primarily from atmospheric nuclear weapons testing, with a smaller contribution from the Chernobyl accident in 1986 (Gwynn *et al.* 2004). Ice core surveys indicate that the deposition of ^{137}Cs from the Chernobyl fallout reached approximately 20 Bq m^{-2} (Pinglot *et al.* 1994). Higher cryoconite values were reported by Łokas *et al.* (2016, 2019) for southwestern and northwestern Spitsbergen, compared with the present study (Fig. 4). Furthermore, Łokas *et al.* (2017a, 2019) noted that the highest ^{137}Cs activity concentrations in tundra and proglacial zone soils were associated with glacier melt processes, with a substantial contribution from cryoconite. Saniewski *et al.* (2000) described higher mean ^{137}Cs activity concentrations in bryophytes and lichens collected from different parts of Svalbard than those observed in glacier mice and bryophytes in the present study (Fig. 4). Activity concentrations of ^{137}Cs are generally higher in selected Arctic vegetation, such as bryophytes and lichens, than in adjacent soils (Gwynn *et al.* 2004). The absence of elevated ^{137}Cs activity concentrations in cryoconite suggests that proglacial sediments in the study area are unlikely to contain high levels of this radionuclide. Additionally, glacier mice collected from Spitsbergen exhibited the lowest ^{137}Cs activity concentrations (Fig. 4) compared with those from Norway and Iceland (Kołtonik *et al.* 2024, 2025).

A similar pattern was observed for ^{210}Pb, as cryoconite exhibited higher activity concentrations than those measured in other matrices. Moreover, variability in ^{210}Pb activity

Polish Polar Research - Accepted Article

This article has been accepted for publication in a future issue of PPRes, but has not been fully edited. Content may change prior to final publication.

concentrations within cryoconite was observed between the Longyearbreen and Foxfonna glaciers and can be attributed to the duration of cryoconite exposure to atmospheric deposition (Łokas *et al.* 2018). Another factor contributing to the higher ^{210}Pb activity concentration observed at Longyearbreen may be the enhanced accumulation of atmospherically derived ^{210}Pb in lower-elevation glaciers (Buda *et al.* 2024). Furthermore, Longyearbreen is smaller (2.5 km^2; Langford *et al.* 2014) than Foxfonna (6 km^2; Rassner *et al.* 2024), which may affect radionuclide accumulation rates. Similar associations have been reported for Alpine glaciers, although at a larger spatial scale (Buda *et al.* 2024). A significant relationship between organic matter content and radionuclide activity concentrations was observed only for ^{210}Pb in cryoconite samples from Foxfonna. Inputs of ^{210}Pb may also originate from anthropogenic sources, with environmental levels enhanced by human activities such as fossil fuel combustion in power plants, agricultural practices, fertilizer production, and vehicular emissions (Uğur *et al.* 2009; Sert *et al.* 2011; Kılıç *et al.* 2014). Although historical emissions from coal combustion in Longyearbyen, located within approximately 5 km from the glacier, could represent a potential additional source of Pb-bearing particles, this hypothesis remains uncertain and requires further verification using complementary tracers. Published data on ^{210}Pb activity concentrations in cryoconite from Svalbard reported by Łokas *et al.* (2016, 2019) indicate higher mean value than those observed in the present study (Fig. 4). In contrast, lower ^{210}Pb activity concentrations have been reported for proglacial and tundra soils at depths of 0.5–2 cm, reaching up to 519 Bq kg^{-1} and 312 Bq kg^{-1}, respectively (Łokas *et al.* 2017a, 2019). Information on ^{210}Pb concentrations in bryophytes from Svalbard is limited. ^{210}Pb activity concentrations in peat profiles are lower than those measured in glacier mice and bryophytes in the present study, with maximum values of up to 180 Bq kg^{-1} in the uppermost 0.5–1 cm layer (Cwanek and Łokas 2022). The mean of ^{210}Pb activity in glacier mice noted for Svalbard is lower than that observed in Norway but higher than that in Iceland (Fig. 4; Kołtonik *et al.* 2024, 2025).

In our study, cryoconite showed a lower mean activity concentration of $^{239+240}$Pu compared to activities observed in glacier mice and bryophytes. Overall, the $^{239+240}$Pu activity concentrations measured in the studied matrices differed from values described in the literature. Łokas *et al.* (2024) presented $^{239+240}$Pu data for cryoconite from Svalbard, reporting a higher mean value of 13.27 Bq kg^{-1} compared with those obtained in the present study. Higher $^{239+240}$Pu activity concentrations were also received in proglacial and tundra soils at depths of 0.5–2.5 cm, with maximum values of 3.89 Bq kg^{-1} and 1.00 Bq kg^{-1}, respectively (Łokas *et al.* 2017a). Similarly, $^{239+240}$Pu activity concentrations in peat profiles, ranging from 0.12 to 0.20 Bq kg^{-1} at a depth of 1–2 cm (Łokas *et al.* 2013), were higher than those

Polish Polar Research - Accepted Article

This article has been accepted for publication in a future issue of PPRes, but has not been fully edited. Content may change prior to final publication.

measured in glacier mice and bryophytes in the present study. Glacier mice in Svalbard exhibit the lowest $^{239+240}$Pu activity concentrations compared with published data from Norway and Iceland (Fig. 4).

The mean ^{240}Pu/^{239}Pu atomic ratios measured in the cryoconite samples (Fig. 4) were slightly below (mean = 0.165, n=15) than the global fallout reference value (~0.18; Kelley *et al.* 1999). Similarly low ratios have previously been reported for cryoconite from Svalbard (mean = 0.145, n = 61; Łokas *et al.* 2024) and for proglacial soils (mean = 0.169, n = 77; Łokas *et al.* 2017b). In contrast, tundra soils exhibited ^{240}Pu/^{239}Pu atomic ratios closer to the global fallout signature (mean = 0.179, n = 80; Łokas *et al.* 2017b). Łokas *et al.* (2017b) suggested that the observed differences between proglacial and tundra soils may be related to the very slow development of tundra soils, resulting in more uniform and homogeneous ^{240}Pu/^{239}Pu atomic ratio. The variation in ^{240}Pu/^{239}Pu atomic ratios observed in the study area between bryophytes collected from moraine and glacier mice is likely attributable to the mixing of distinct plutonium isotopic signatures within the moraine environment. The relatively low ^{240}Pu/^{239}Pu atomic ratios observed in some Svalbard samples may indicate contributions from sources other than global fallout, potentially including material associated with historical nuclear detonations at the Novaya Zemlya and Semipalatinsk test sites. Consistent with this interpretation, Wendel *et al.* (2013) reported low ^{240}Pu/^{239}Pu atomic ratios in ice cores from north-eastern Svalbard, suggesting that tropospheric transport of debris from the Novaya Zemlya and Semipalatinsk test sites contributed to radionuclide deposition in the region. Furthermore, trajectory modelling by Wendel *et al.* (2013) indicated that radioactive debris from Semipalatinsk was likely transported to Svalbard.

Spatial variability in precipitation (mean annual precipitation of 191 mm at Longyearbyen; Førland *et al.* 2011) may partly explain differences in glacier contamination, as coastal areas of Svalbard (*e.g.*, Kaffiøyra area; Łokas *et al.* 2019) receive approximately twice as much precipitation as in inland regions (Førland *et al.* 2011). Post-depositional processes, particularly those associated with cryoconite hole formation and subsequent material transport within the glacier, appear to exert a stronger influence on some radionuclide contamination levels (Łokas *et al.* 2019). It is confirmed by different radionuclide contamination patterns (*e.g.*, ^{137}Cs) observed in the two studied glaciers (Longyearbreen and Foxfonna).

The relatively low activity concentrations of radionuclides observed in the investigated samples suggest that radionuclide inventories in the studied glacier compartments are unlikely to represent a major contamination source based on concentration alone. However, assessment of potential downstream impacts would require information on

Polish Polar Research - Accepted Article

This article has been accepted for publication in a future issue of PPRes, but has not been fully edited. Content may change prior to final publication.

radionuclide inventories, glacier meltwater fluxes, and contaminant transport rates. In contrast, data reported for other glaciers in Svalbard, based on radionuclide concentrations in cryoconite and proglacial soils, indicate a higher environmental risk (Łokas *et al.* 2016, 2017a, 2017b, 2019, 2024; Clason *et al.* 2023).

Conclusions

This study provides the first assessment of radionuclide accumulation in glacier mice in Svalbard and the first direct comparison of radionuclide concentrations between glacier mice and cryoconite from a High Arctic glacier. The results indicate that radionuclide accumulation is likely influenced by glacier-specific environmental conditions, including physical and spatial characteristics and the availability of different accumulation matrices (cryoconite versus bryophytes). Glacier mice examined in this study were identified as *Sanionia nivalis*, and *Hygrohypnella polaris*, providing additional information on the biological composition of these unique glacier aggregates. The measured $^{240}Pu/^{239}Pu$ atomic ratios were largely consistent with global atmospheric fallout while suggesting a minor contribution from regional nuclear weapons testing.

These findings demonstrate that glacier mice represent a previously overlooked biological compartment involved in radionuclide cycling within glacier ecosystems. Their capacity to integrate radionuclides derived from atmospheric deposition and glacier processes highlights their potential as complementary biomonitors for assessing contaminant in rapidly changing Arctic glacier environments.

Polish Polar Research - Accepted Article

Acknowledgements

This research was supported by the statutory research funds of the Institute of Nuclear Physics Polish Academy of Sciences. We are indebted to Lars Hedenäs (Swedish Museum of Natural History) for revision of some specimens determination. We sincerely thank the reviewers for their constructive comments and valuable suggestions, which have helped us improve the quality of our manuscript.

Supplementary materials

Table S1. Activity concentrations of natural (^{210}Pb) and anthropogenic (^{137}Cs, $^{239+240}Pu$) radionuclides and atomic ratios in glacier mice, bryophytes and cryoconite at Spitsbergen glaciers.

Table S2. Quality control of gamma spectrometry. IAEA (International Atomic Energy Agency) activity concentrations of radionuclides in IAEA world-wide proficiency tests compared to those determined using a planar BEGe™ Canberra gamma counter at the Central Mining Institute – National Research Institute.

This article has been accepted for publication in a future issue of PPRes, but has not been fully edited. Content may change prior to final publication.

Table S3. Quality control results of the methods of mass spectrometry with IAEA certified standard.

References

ACIA 2005. *Arctic Climate Impact Assessment. ACIA Overview report*. Cambridge University Press, Cambridge, https://www.amap.no/documents/doc/arctic-arctic-climate-impact-assessment/796.

Baccolo G., Łokas E., Gaca P., Massabò D., Ambrosini,R., Azzoni R.S., Clason C., Di Mauro B., Franzetti A., Nastasi M., Prata M., Prati P., Previtali E., Delmonte B. and Maggi V. 2020. Cryoconite: an efficient accumulator of radioactive fallout in glacial environments. *The Cryosphere* 14: 657–672, doi: 10.5194/tc-14-657-2020.

Belkina O.A. and Mavlyuduv B.R. 2011. Mosses on glaciers of Spitzbergen. *Botanicheskiy Zhurnal* 96: 582–596 (in Russian with English summary).

Belkina O.A. and Vilnet A.A. 2015. Some aspects of the moss population development on the Svalbard glaciers. *Czech Polar Reports* 5: 160–175.

Buda J., Łokas E., Pietryka M., Richter D., Magowski W., Iakovenko N.S., Porazinska D.L., Budzik T., Grabiec M., Grzesiak J., Klimaszyk P. and Zawierucha K. 2020. Biotope and biocenosis of cryoconite hole ecosystems on ecology glacier in the maritime Antarctic. *Science of the Total Environment* 724: 138112, doi: 10.1016/j.scitotenv.2020.138112.

Buda J., Błażej S., Ambrosini R., Scotti R., Pittino F., Sala D., Zawierucha K. and Łokas E. 2024. The surface of small glaciers as radioactive hotspots: concentration of radioisotopes during predicted intensive melting in the Alps. *Journal of Hazardous Materials* 476: 135083, doi: 10.1016/j.jhazmat.2024.135083.

Bouville A. 2020. Fallout from Nuclear Weapons Tests: Environmental, Health, Political, and Sociological Considerations. *Health Physics* 118: 360–381, doi: 10.1097/HP.0000000000001237.

Burakowska A., Kubicki M., Mysłek-Laurikainen B., Piotrowski M., Trzaskowska H. and Sosnowiec R. 2021. Concentration of ^{7}Be, ^{210}Pb, ^{40}K, ^{137}Cs, ^{134}Cs radionuclides in the ground layer of the atmosphere in the polar (Hornsund, Spitsbergen) and mid-latitudes (Otwock-Świder, Poland) regions. *Journal of Environmental Radioactivity* 240: 106739, doi: 10.1016/j.jenvrad.2021.106739.

Chmiel S., Reszka M. and Rysiak A. 2009. Heavy metals and radioactivity in environmental samples of the Scott Glacier Region on Spitsbergen in summer 2005. *Quaestiones Geographicae* 28a/1.

Christiansen H.H., French H.M. and Humlum O. 2005. Permafrost in the Gruve-7 mine, Adventdalen, Svalbard. *Norsk Geografisk Tidsskrift - Norwegian Journal of Geography* 59: 109–115, doi: 10.1080/00291950510020592.

Christiansen H.H., Matero I.S.O., Baddeley L., Holmén K., Hoppe C.J.M., Loonen M.J.J.E., Storvold R., Vitale V., Zaborska A. and Lihavainen H. 2024. Developing the Svalbard Integrated Arctic

Polish Polar Research - Accepted Article

Earth Observing System (SIOS). *Earth System Dynamics* 15: 933–946, doi: 10.5194/esd-15-933-2024.

Clason C.C., Baccolo G., Łokas E., Owens P.N., Wachniew P., Millward G.E., Taylor A., Blake W.H., Beard D.B., Poniecka E., Selmes N., Bagshaw E.A., Cook J., Fyfe R., Hay M., Land D., Takeuchi N., Nastasi M., Sisti M., Pittino F., Franzetti A., Ambrosini R. and Di Mauro, B. 2023. Global variability and controls on the accumulation of fallout radionuclides in cryoconite. *Science of the Total Environment* 894: 164902, doi: 10.1016/j.scitotenv.2023.164902.

Cook J., Edwards A., Takeuchi N. and Irvine-Fynn T. 2016. Cryoconite: the dark biological secret of the cryosphere. *Progress in Physical Geography: Earth and Environment* 40: 66–111, doi: 10.1177/0309133315616574.

Coulson S.J. 2013. The terrestrial invertebrate fauna of the Svalbard archipelago in a changing world: history of research and challenges. *The Canadian Entomologist* 145: 131–146, doi: 10.4039/tce.2012.110.

Coulson S.J. and Midgley N.G. 2012. The role of glacier mice in the invertebrate colonisation of glacial surfaces: the moss balls of the Falljökull, Iceland. *Polar Biology* 35: 1651–1658, doi: 10.1007/s00300-012-1205-4.

Crosta A., Valle B., Caccianiga M., Gobbi M., Ficetola F.G., Pittino F., Franzetti A., Azzoni R.S., Lencioni V., Senese A., Corlatti L., Buda J., Poniecka E., Novotná Jaroměřská T., Zawierucha K. and Ambrosini R. 2024. Ecological interactions in glacier environments: A review of studies on a model Alpine glacier. *Biological Reviews* 100: 227–244, doi: 10.1111/brv.13138.

Cwanek A. and Łokas E. 2022. Deposition chronologies in a peat bog from Spitsbergen (High Arctic) using the ^{210}Pb dating method. *Polish Polar Research* 43: 291–310, doi: 10.24425/ppr.2022.143310.

Cwanek A., Łokas E., Dinh C.N., Zagórski P., Singh S.M., Szufa K. and Tomankiewicz E. 2020. ^{90}Sr level and behaviour in the terrestrial environment of Spitsbergen. *Journal of Radioanalytical and Nuclear Chemistry* 327: 485–494, doi: 10.1007/s10967-020-07492-z.

Cwanek A., Burakowska A., Nalichowska E., Długosz-Lisiecka M., Kubicki M., Wawrzyniak T., Łokas E., Gryziński M. and Lubera G. 2026. Unprecedented radioactive pollution in Spitsbergen air – first data as of 21st century. *Atmospheric Chemistry and Physics* 26: 5839–5860, doi: 10.5194/acp-26-5839-2026.

Dowdall M., Gerland S. and Lind B. 2003. Gamma-emitting natural and anthropogenic radionuclides in the terrestrial environment of Kongsfjord, Svalbard. *Science of the Total Environment* 305: 229–240, doi: 10.1016/S0048-9697(02)00478-3.

Førland E.J., Benestad R., Hanssen-Bauer I., Haugen J.E. and Skaugen T.E. 2011. Temperature and precipitation development at Svalbard 1900–2100. *Advances in Meteorology* 893790, doi: 10.1155/2011/893790.

Polish Polar Research - Accepted Article

This article has been accepted for publication in a future issue of PPRes, but has not been fully edited. Content may change prior to final publication.

García-Tenorio R. 2018. $^{240}Pu/^{239}Pu$ atomic ratio as a fingerprint of local and tropospheric fallout due to events involving nuclear weapons: A review. *Journal of Radiation and Nuclear Applications* 3: 65–77, doi: 10.18576/jrna/030201.

Gwynn J.P., Dowdall M., Davids C., Selnæs Ø.G. and Lind B. 2004. The radiological environment of Svalbard. *Polar Research* 23: 167–180, doi: 10.3402/polar.v23i2.6277.

Harmens H., Norris D., Sharps K., Mills G., Alber R., Aleksiayenak Y., Blum O., Cucu-Man S.M., Dam M., De Temmerman L., Ene, A., Fernández, J.A., Martinez-Abaigar, J., Frontasyeva, M., Godzik, B., Jeran, Z., Lazo, P., Leblond, S., Liiv, S., Magnússon, S.H., Maňkovská, B., Pihl Karlsson, G., Piispanen, J., Poikolainen, J., Santamaria, J.M., Skudnik, M., Spiric, Z., Stafilov, T., Steinnes, E., Stihi, C., Suchara, I., Thöni, L., Todoran, R., Yurukova, L. and Zechmeister H.G. 2015. Heavy metal and nitrogen concentrations in mosses are declining across Europe whilst some "hotspots" remain in 2010. *Environmental Pollution* 200: 93–104, doi: 10.1016/j.envpol.2015.01.036.

Hedenäs L. 1989. The genus *Sanionia* (Musci) in Northwestern Europe, a taxonomic revision. *Annales Botanici Fennici* 26: 399–419.

Hedenäs L. 2014. *Sanionia*. *In*: Flora of North America Editorial Committee (ed.) *Flora of North America north of Mexico. Vol. 28. Bryophyta, part 2*. Oxford University Press, New York and Oxford: 306–310.

Hedenäs L., Reisborg C. and Hallingbäck T. 2014. *The National Key to Sweden's Flora and Fauna. Mosses: Hookeria Mosses to Anomodon Mosses. Bryophyta: Hookeria–Anomodon.* Uppsala: ArtDatabanken, Sveriges lantbruksuniversitet (SLU) (in Swedish).

Hotaling S., Bartholomaus T.C. and Gilbert S.L. 2020. Rolling stones gather moss: movement and longevity of moss balls on an Alaskan glacier. *Polar Biology* 43: 735–744, doi: 10.1038/s41559-020-1163-0.

Ignatiuk D., Błaszczyk M., Budzik T., Grabiec M., Jania J.A., Kondracka M., Laska M., Małarzewski Ł. and Stachnik Ł. 2022. A decade of glaciological and meteorological observations in the Arctic (Werenskioldbreen, Svalbard). *Earth System Science Data* 14: 2487–2500, doi: 10.5194/essd-14-2487-2022.

Jamieson D.W. 2014. *Hygrohypnum*. *In*: Flora of North America Editorial Committee (ed.) *Flora of North America north of Mexico*. *Vol. 28. Bryophyta, part 2*. Oxford University Press, New York and Oxford: 269–282.

Jania J., Majchrowska E., Ignatiuk D., Marszałek H. and Wąsik M. 2015. Seasonal and interannual variability in runoff from the Werenskioldbreen catchment, Spitsbergen. *Polish Polar Research* 36: 197–224, doi: 10.1515/popore-2015-0014.

Kelley J., Bond L. and Beasley T. 1999. Global distribution of Pu isotopes and ^{237}Np. *Science of the Total Environment* 237: 483–500, doi: 10.1016/S0048-9697(99)00160-6.

Polish Polar Research - Accepted Article

This article has been accepted for publication in a future issue of PPRes, but has not been fully edited. Content may change prior to final publication.

Kılıç Ö., Belivermiş M., Cotuk Y. and Topçuoğlu S. 2014. Radioactivity concentrations in mussel (*Mytilus galloprovincialis*) of Turkish Sea coast and contribution of sup ^{210}Po to the radiation dose. *Marine Pollution Bulletin* 80: 325–329, doi: 10.1016/j.marpolbul.2013.12.037.

Kłos A., Ziembik Z., Rajfur M., Dołhańczuk-Śródka A., Bochenek Z., Bjerke J.W. and Godyń P. 2017. The origin of heavy metals and radionuclides accumulated in the soil and biota samples collected in Svalbard, near Longyearbyen. *Ecological Chemistry and Engineering S* 24: 223–238, doi: 10.1515/eces-2017-0015.

Kołtonik K., Zawierucha K., Wojciechowski K., Mróz T., Niedzierski P., Souza-Kasprzyk J., Wierzgoń M., Olabode K., Cwanek A., Sala D., Yde J.C., Wachniew P. and Łokas E. 2024. Glacier mice as a temporary sink for fallout radionuclides and heavy metals on the Norwegian glacier Austerdalsbreen. *Science of the Total Environment* 949: 175109, doi: 10.1016/j.scitotenv.2024.175109.

Kołtonik K., Wojciechowski K., Sala D., Raszka K., Samolej K., Bonczyk M., Wachniew P. and Łokas E. 2025. Exceptional plutonium accumulation in glacier mice and cryoconite in Icelandic glaciers. *Science of the Total Environment* 999: 180370, doi: 10.1016/j.scitotenv.2025.180370.

Krey P.W. 1967. Atmospheric Burnup of a Plutonium-238 Generator. *Science* 158: 769–771, doi: 10.1126/science.158.3802.769.

Langford H.J., Irvine-Fynn T.D.L., Edwards A., Banwart S.A. and Hodson A.J. 2014. A spatial investigation of the environmental controls over cryoconite aggregation on Longyearbreen glacier, Svalbard. *Biogeosciences* 1: 5365–5380, doi: 10.5194/bg-11-5365-2014.

Lencioni V., Franceschini A., Paoli F., Lutton, A., Olesik, J. and Gabrielli P. 2023. Metal enrichment in ice-melt water and uptake by chironomids as possible legacy of World War One in the Italian Alps. *Chemosphere* 340: 139757, doi: 10.1016/j.chemosphere.2023.139757.

Lönnell N., Hassel K., Goldberg I., Huttunen S., Bjarnason Á.H., Blom H.H., Hallingbäck T., Hedenäs L., Høitomt T., Pihlaja K., Prestø T., Syrjänen K., Söderström L., Ulvinen T. and Weibull H. 2025. An annotated checklist of bryophytes of the Nordic countries. *Lindbergia* 2025: e025337, doi: 10.25227/linbg.025337.

Łokas E., Ketterer M., Mietelski J.W., Kleszcz K., Wachniew P., Michalska S. and Miecznik M. 2013. Sources and vertical distribution of ^{137}Cs, ^{238}Pu, $^{239+240}$Pu and ^{241}Am in peat profiles from southwest Spitsbergen. *Applied Geochemistry* 28: 100–108, doi: 10.1016/j.apgeochem.2012.10.027.

Łokas E., Bartmiński P., Wachniew P., Mietelsk J.W., Kawiak T. and Srodoń J. 2014. Sources and pathways of artificial radionuclides to soils at a High Arctic site. *Environmental Science and Pollution Research* 21: 12479–12493, doi: 10.1029/2004GL022191.

Łokas E., Zaborska A., Kolicka M., Różycki M. and Zawierucha K. 2016. Accumulation of atmospheric radionuclides and heavy metals in cryoconite holes on an Arctic glacier. *Chemosphere* 160: 162–172, doi: 10.1016/j.chemosphere.2016.06.051.

Polish Polar Research - Accepted Article

This article has been accepted for publication in a future issue of PPRes, but has not been fully edited. Content may change prior to final publication.

Łokas E., Wachniew P., Jodłowski P. and Gąsiorek M. 2017a. Airborne radionuclides in the proglacial environment as indicators of sources and transfers of soil material. *Journal of Environmental Radioactivity* 178–179: 193–202, doi: 10.1016/j.jenvrad.2017.08.018.

Łokas E., Mietelski J.W., Anczkiewicz R. and Kierepko R. 2017b. Variations in Pu isotopic composition in soils from the Spitsbergen (Norway): Three potential pollution sources of the Arctic region. *Chemosphere* 178: 231–238, doi: 10.1016/j.chemosphere.2017.03.054.

Łokas E., Zawierucha K., Cwanek A., Szufa K., Gaca P., Mietelski J.W. and Tomankiewicz E. 2018. The sources of high airborne radioactivity in cryoconite holes from the Caucasus (Georgia). *Scientific Reports* 8: 10802, doi: 10.1038/s41598-018-29076-4.

Łokas E., Zaborska A., Sobota I., Gaca P., Milton J.A., Kocurek P. and Cwanek A. 2019. Airborne radionuclides and heavy metals in high Arctic terrestrial environment as the indicators of sources and transfers of contamination. *The Cryosphere* 13: 2075–2086, doi: 10.5194/tc-13-2075-2019.

Łokas E., Baccolo G., Cwanek A., Buda J., Kołtonik K., Takeuchi N., Wachniew P., Clason C., Zawierucha K., Beard B.B., Ambrosini R., Pittino F., Franzetti A., Owens P.N., Nastasi M., Sisti M. and Di Mauro B. 2024. Isotopic signature of plutonium accumulated in cryoconite on glaciers worldwide. *Science of the Total Environment* 951: 175356, doi: 10.1016/j.scitotenv.2024.175356.

Major H. and Nagy J. 1972. *Geology of the Adventdalen map area: with a geological map, Svalbard 1: 100 000*. Norsk Polarinstitutt Skrifter No. 138, Oslo.

Osuch M. and Wawrzyniak T. 2017. Inter- and intra-annual changes in air temperature and precipitation in western Spitsbergen. *International Journal of Climatology* 37: 3082–3097, doi: 10.1002/joc.4901.

Paatero J., Vira J., Siitari-Kauppi M., Hatakka J., Holmén K. and Viisanen Y. 2012. Airborne fission products in the high Arctic after the Fukushima nuclear accident. *Journal of Environmental Radioactivity* 114: 41–47, doi: 10.1016/j.jenvrad.2011.12.027.

Pinglot J.F., Pourchet M., Lefauconnier B., Hagen J.O., Vaikmae R., Punning J.M., Watanabe O., Takahashi S. and Kameda T. 1994. Natural and artificial radioactivity in the Svalbard glaciers. *Journal of Environmental Radioactivity* 25: 161–176, doi: 10.1016/0265-931X(94)90013-2.

Rassner S.M.E., Cook J.M., Mitchell A.C., Stevens I.T., Irvine-Fynn T.D.L., Hodson A.J. and Edwards A. 2024. The distinctive weathering crust habitat of a High Arctic glacier comprises discrete microbial micro-habitats. *Environmental Microbiology* 26: e16617, doi: 10.1111/1462-2920.16617.

Rozwalak P., Podkowa P., Buda J., Niedzielski P., Kawecki S., Ambrosini R., Azzoni R.S., Baccolo G., Ceballos J.L., Cook J., DiMauro B., Ficetola G.F., Franzetti A., Ignatiuk D., Klimaszyk P., Łokas E., Ono M., Parnikoza I., Pietryka M., Pittino F., Poniecka E., Porazinska D.L., Richter D., Schmidt S.K., Sommers P., Souza-Kasprzyk J., Stibal M., Szczuciński W., Uetake J., Wejnerowski Ł., Yde J.C., Takeuchi N. and Zawierucha K. 2022. Cryoconite – from minerals

Polish Polar Research - Accepted Article

and organic matter to bioengineered sediments on glacier's surfaces. *Science of the Total Environment* 807: 150874, doi: 10.1016/j.scitotenv.2021.150874.

Salminen-Paatero S., Vira J. and Paatero J. 2020. Measurements and modeling of airborne plutonium in subarctic Finland between 1965 and 2011. *Atmospheric Chemistry and Physics* 20: 5759–5769, doi: 10.5194/acp-20-5759-2020.

Saniewski M., Wietrzyk-Pełka P., Zalewska T., Olech M. and Węgrzyn M.H. 2020. Bryophytes and lichens as fallout originated radionuclide indicators in the Svalbard Archipelago (High Arctic). *Polar Science* 25: 100536, doi: 10.1016/j.polar.2020.100536.

Schuler T.V., Kohler J., Elagina N., Hagen J.O.M., Hodson A.J., Jania J.A., Kääb A.M., Luks B., Małecki J., Moholdt G., Pohjola V.A., Sobota I. and Van Pelt W.J. 2020. Reconciling Svalbard glacier mass balance. *Frontiers in Earth Science* 8: 156, doi: 10.3389/feart.2020.00156.

Schuler T.V., Benestad R.E., Isaksen K., Kierulf H.P., Kohler J., Moholdt G. and Schmidt L.S. 2025. Svalbard's 2024 record summer: An early view of Arctic glacier meltdown? *Proceedings of the National Academy of Sciences U.S.A.* 122: e2503806122, doi: 10.1073/pnas.2503806122.

Senger K., Betlem P., Braathen A., Olaussen S. and Sand G. 2025. Longyearbyen CO_2 lab project–from a vision of a CO_2-neutral Svalbard to a geoscience data eldorado. *Arctic Science* 11: 1–26, doi: 10.1139/as-2024-0019.

Serreze M.C. and Barry R.G. 2011. Processes and impacts of Arctic amplification: A research synthesis. *Global and Planetary Change* 77: 85–96, doi: 10.1016/j.gloplacha.2011.03.004.

Sert E., Uğur A., Özden B., Saç M. and Camgöz B. 2011. Biomonitoring of ^{210}Po and ^{210}Pb using lichens and mosses around coal-fired power plants in Western Turkey. *Journal of Environmental Radioactivity* 102: 535–542, doi: 10.1016/j.jenvrad.2011.02.005.

Smith E., Clason C.C., Millward G., Taylor A. and Fyfe R. 2024. Radiological and elemental composition of cryoconite and glacier mice from Vatnajokull, Iceland. *Science of the Total Environment* 951: 175828, doi: 10.1016/j.scitotenv.2024.175828.

Stocki T.J. 2026. Historical insights from past SMRs used in nuclear propulsion and electricity generation in remote locations. *International Journal of Radiation Biology* 1–12, doi: 10.1080/09553002.2026.2629246.

Takeuchi N., Kohshima S., Shiraiwa T. and Kubota K. 2001. Characteristics of cryoconite (surface dust on glaciers) and surface albedo of a Patagonian glacier, Tyndall Glacier, Southern Patagonia Icefield. *Bulletin of Glaciological Research* 18: 65–69.

Taylor R.N., Warneke T., Milton J.A., Croudace I.W., Warwick P.E. and Nesbitt, R.W. 2001. Plutonium isotope ratio analysis at femtogram to nanogram levels by multicollector ICP-MS *Journal of Analytical Atomic Spectrometry* 16: 279–284, doi: 10.1039/b009078f.

Uetake J., Samyn D., Anguma S. and Takeuchi N. 2022. spatial distribution of unique biological communities and their control over surface reflectivity of the Stanley glacier, Uganda. *Frontiers in Earth Science* 10: 740998, doi: 10.3389/feart.2022.740998.

Polish Polar Research - Accepted Article

Uğur A., Özden B., Yener G., Saç M., Kurucu Y., Altınbaş Ü. and Bolca M. 2009. Distributions of ^{210}Pb around a uraniferous coal-fired power plant in Western Turkey. *Environmental Monitoring and Assessment* 149: 195–200, doi: 10.1007/s10661-008-0193-x.

United Nations Scientific Committee on the Effects of Atomic Radiation (UNSCEAR) 2000. Exposures to the public from man-made sources of radiation. *In: Sources and Effects of Ionizing Radiation, United Nations Scientific Committee on the Effects of Atomic Radiation UNSCEAR 2000 Report to the General Assembly, with Scientific Annexes: Volume I: Sources*. New York, United Nations: Annex C: 157–292, https://www.unscear.org/unscear/uploads/documents/unscear-reports/UNSCEAR_2000_Report_Vol.I.pdf.

Wawrzyniak T. and Osuch M. 2020. A 40-year High Arctic climatological dataset of the Polish Polar Station Hornsund (SW Spitsbergen, Svalbard). *Earth System Science Data* 12: 805–815, doi: 10.5194/essd-12-805-2020.

Wendel C.C., Fifield L.K., Oughto, D.H., Lind O.C., Skipperud L., Bartnicki J., Tims S.G., Høibråten S. and Salbu B. 2013. Long-range tropospheric transport of uranium and plutonium weapons fallout from Semipalatinsk nuclear test site to Norway. *Environment International* 59: 92–102, doi: 10.1016/j.envint.2013.05.017.

Yde J.C., Riger-Kusk M., Christiansen H.H., Knudsen N.T. and Humlum O. 2008. Hydrochemical characteristics of bulk meltwater from an entire ablation season, Longyearbreen, Svalbard. *Journal of Glaciology* 54: 259–272, doi: 10.3189/002214308784886234.

Zaborska A. 2017. Sources of ^{137}Cs to an Arctic fjord (Hornsund, Svalbard). *Journal of Environmental Radioactivity* 180: 19–26, doi: 10.1016/j.jenvrad.2017.09.021.

Zawierucha K., Buda J. and Nawrot A. 2019. Extreme weather event results in the removal of invertebrates from cryoconite holes on an Arctic valley glacier (Longyearbreen, Svalbard). *Ecological Research* 34: 370–379, doi: 10.1111/1440-1703.1276.

Zawierucha K., Szudarek-Trepto N., Laniecki R., Valle B., Mikołajczyk M., Trzebny A., Nahimova O., Wierzgoń M., Kaźmierski A., Niedbała W., Rutkowski T., Kołtonik K., Łokas E., Ficetola G.F., Konwerski S., Stachowiak M., Yde J.C. and Calhim S. 2026. Morphological and molecular inventory of invertebrates reveals a unique faunal diversity in glacier mice. *Journal of Zoology* 328: 384–401, doi: 10.1111/jzo.70105.

Polish Polar Research - Accepted Article

This article has been accepted for publication in a future issue of PPRes, but has not been fully edited. Content may change prior to final publication.

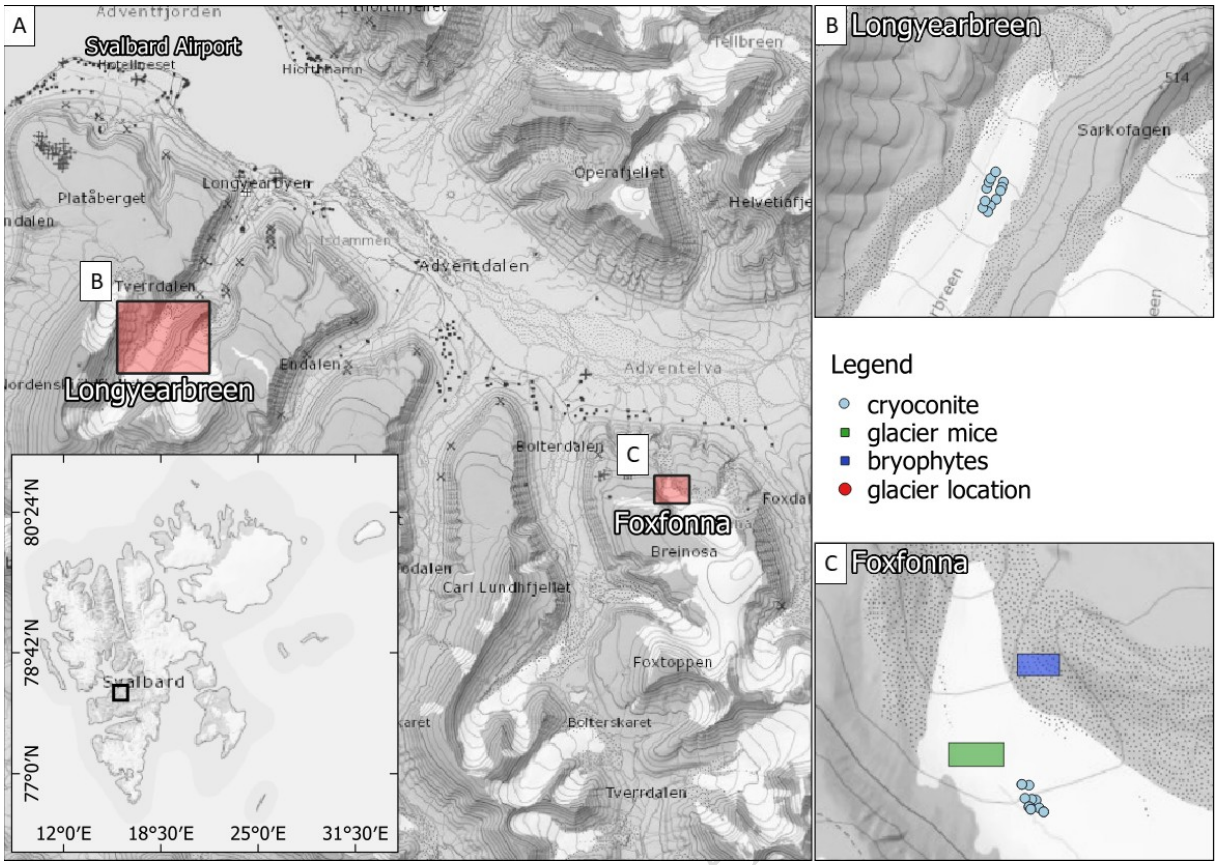


Fig. 1. Map of the study area (**A**), showing the locations of Longyearbreen (**B**) and Foxfonna (**C**) glaciers, along with sampling sites. Image source: https://geodata.npolar.no.

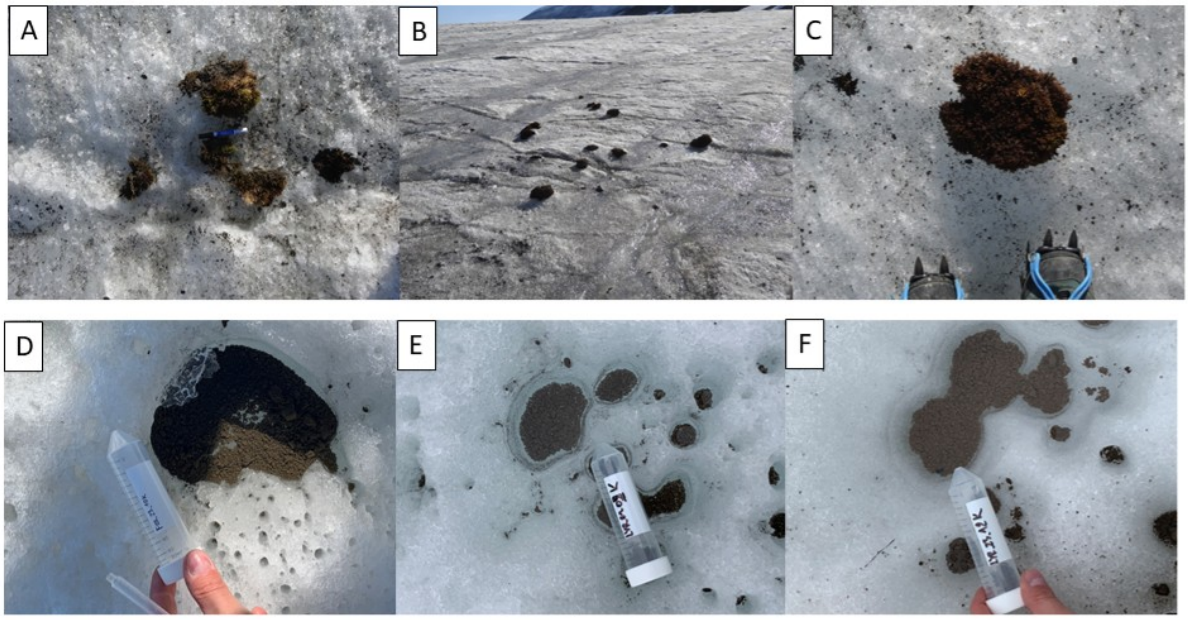


Fig 2. Photographs: (**A**–**C**) a glacier mice colony at Foxfonna; (**D**) cryoconite at Foxfonna and (**E**, **F**) cryoconite at Longyearbreen.

This article has been accepted for publication in a future issue of PPRes, but has not been fully edited. Content may change prior to final publication.

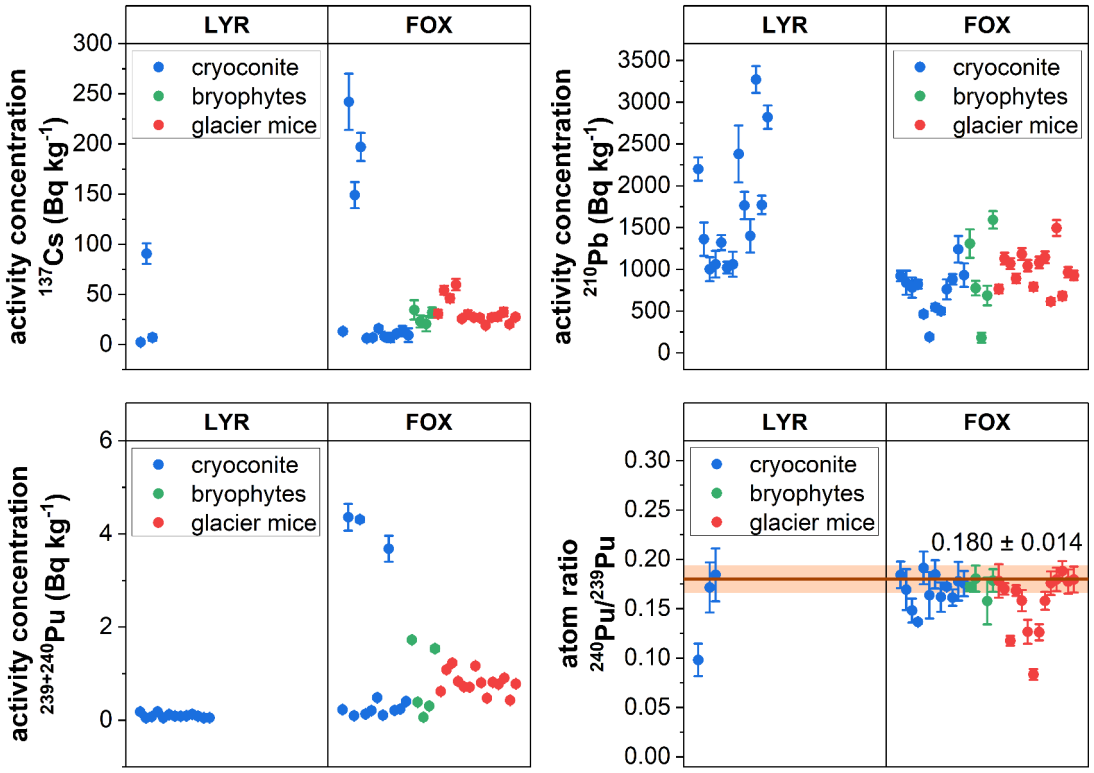


Fig. 3. Activity concentrations and atomic ratio of each sample collected at Spitsbergen glaciers. LYR - Longyearbreen, FOX - Foxfonna. The red horizontal line with shadowed uncertainty in the lower right panel represents the reference Global Fallout ratio.

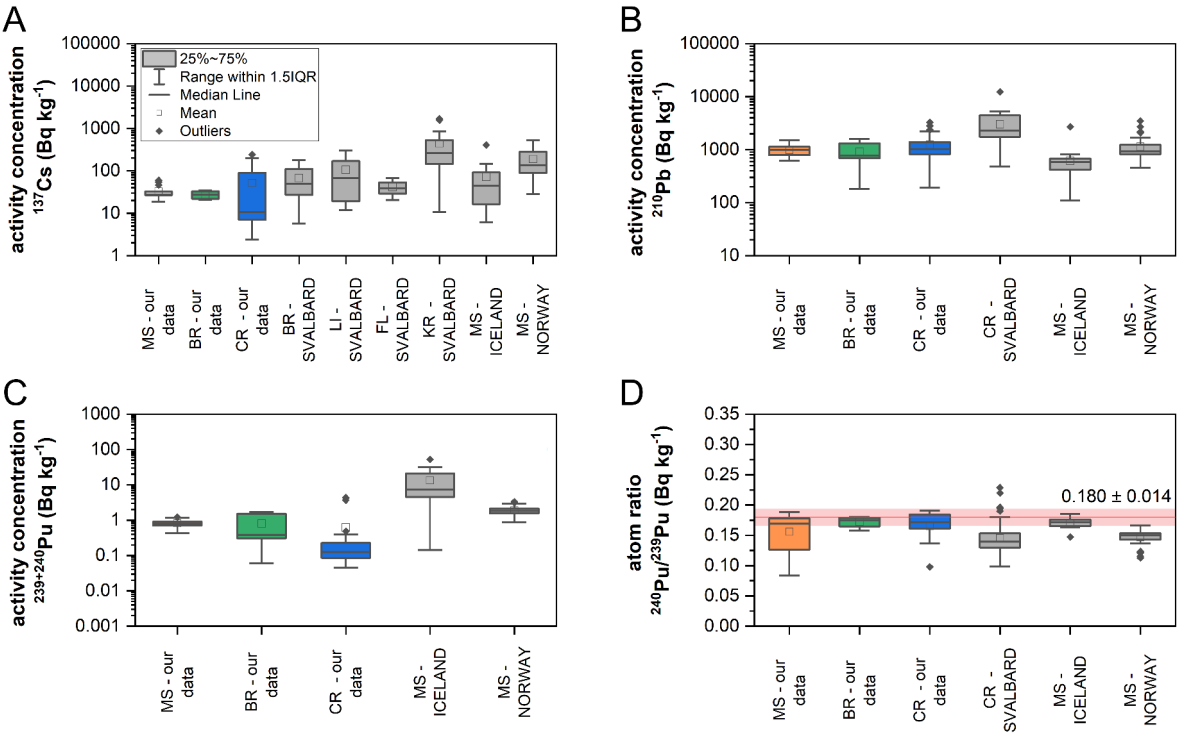


Fig. 4. Activity concentrations and atomic ratios in glacier mice, cryoconite and sediments at the studied glaciers compared to published data from Svalbard, Iceland and Norway. MS - glacier mice, BR- bryophytes, LI - lichens, FL - flowering plants and CR - cryoconite. (**A**) Comparative data for

This article has been accepted for publication in a future issue of PPRes, but has not been fully edited. Content may change prior to final publication.

^{137}Cs include: BR - SVALBARD (Saniewski *et al.* 2020; Gwynn *et al.* 2004), LI - SVALBARD (Saniewski *et al.* 2020; Gwynn *et al.* 2004), FL - SVALBARD (Gwynn *et al.* 2004); CR - SVALBARD (Łokas *et al.* 2016, 2019), MS - ICELAND (Smith *et al.* 2024; Kołtonik *et al.* 2025), MS - NORWAY (Kołtonik *et al.* 2024). (**B**) Comparative data for ^{210}Pb include: CR - SVALBARD (Łokas *et al.* 2016, 2019), MS - ICELAND (Smith *et al.* 2024; Kołtonik *et al.* 2025), MS - NORWAY (Kołtonik *et al.* 2024). (**C**) Comparative data for $^{239+240}$Pu include: MS - ICELAND (Kołtonik *et al.* 2025), MS - NORWAY (Kołtonik *et al.* 2024). (**D**) Comparative data for ^{240}Pu/^{239}Pu include: CR - SVALBARD (Łokas *et al.* 2024), MS - ICELAND (Kołtonik *et al.* 2025), MS - NORWAY (Kołtonik *et al.* 2024). The red horizontal line with shadowed uncertainty in the lower right panel represents the reference Global Fallout ratio.

Polish Polar Reseach - Accepted Article

Table S1. Activity concentrations of natural (^{210}Pb) and anthropogenic (^{137}Cs, $^{239+240}$Pu) radionuclides and atomic ratios in glacier mice, bryophytes and cryoconite at Spitsbergen glaciers. All uncertainties are reported as 1σ (k = 1). Sample **in bold** is represented by organic (o.f.) and sediment fractions (s.f.).

Sample Name	Sample Type	Altitude [m	Latitude	Longitude	Activity concentration (Bq kg^{-1})	Radioisotope ratio	Organic

		a.s.l.]			^{137}Cs	^{210}Pb	$^{239+240}$Pu	^{240}Pu/ ^{239}Pu	matter [%]
LYR_21_01	cryoconite	NA	NA	NA	< 5.8	2200 ± 70	0.178 ± 0.009	0.0981 ± 0.0164	5.7
LYR_23_01	cryoconite	312	78.1846	15.5198	< 5.0	1360 ± 100	0.049 ± 0.006	-	5.5
LYR_23_02	cryoconite	313	78.1844	15.5194	2.4 ± 0.8	1001 ± 72	0.075 ± 0.006	0.1714 ± 0.0254	5.7
LYR_23_03	cryoconite	317	78.1842	15.5191	90.6 ± 5.1	1060 ± 80	0.182 ± 0.015	0.1842 ± 0.0268	6.4
LYR_23_04	cryoconite	324	78.1837	15.5179	< 5.7	1320 ± 45	0.046 ± 0.008	-	5.2
LYR_23_05	cryoconite	332	78.1833	15.5164	< 4.3	1020 ± 35	0.120± 0.015	-	5.0
LYR_23_06	cryoconite	337	78.1830	15.5156	< 6.0	1060 ± 75	0.089 ± 0.008	-	7.9
LYR_23_07	cryoconite	338	78.1832	15.5143	< 5.0	2380 ± 170	0.084 ± 0.008	-	6.3
LYR_23_08	cryoconite	331	78.1836	15.5149	7 ± 1.6	1763 ± 82	0.090 ± 0.01	-	5.9
LYR_23_09	cryoconite	323	78.1843	15.5153	< 6.0	1400 ± 100	0.126 ± 0.017	-	6.0
LYR_23_10	cryoconite	320	78.1846	15.5159	< 14	3270 ± 80	0.085 ± 0.012	-	5.9
LYR_23_11	cryoconite	316	78.1848	15.5164	< 3.2	1770 ± 55	0.050 ± 0.007	-	6.1
LYR_23_12	cryoconite	310	78.1852	15.5177	< 14	2820 ± 70	0.051 ± 0.006	-	4.5
FOX_23_01	cryoconite	453	78.1475	16.1143	13.1 ± 1.3	920 ± 32	0.226 ± 0.008	0.1842 ± 0.0135	8.1
FOX_23_02	cryoconite	454	78.1474	16.1147	242 ± 14	839 ± 73	4.357 ± 0.288	0.1693 ± 0.0207	5.8
FOX_23_03	cryoconite	455	78.1473	16.1151	149 ± 6.5	780 ± 60	0.095 ± 0.007	0.1480 ± 0.0122	4.9
FOX_23_04	cryoconite	455	78.1473	16.1151	197 ± 7	822 ± 26	4.308 ± 0.057	0.1366 ± 0.0021	5.3
FOX_23_05	cryoconite	440	78.1476	16.1139	6.2 ± 0.9	464 ± 17	0.131 ± 0.005	0.1913 ± 0.0166	6.1
FOX_23_06	cryoconite	429	78.1479	16.1136	6.9 ± 1.2	190 ± 15	0.206 ± 0.011	0.1636 ± 0.0234	3.3
FOX_23_07	cryoconite	424	78.1479	16.1129	15.9 ± 1.4	546 ± 21	0.484 ± 0.031	0.1846 ± 0.0143	4.7
FOX_23_08	cryoconite	425	78.1476	16.1132	7.9 ± 1.2	500 ± 20	0.107 ± 0.005	0.1617 ± 0.0149	6.9
FOX_23_09	cryoconite	429	78.1474	16.1136	7.1 ± 2.4	760 ± 60	3.679 ± 0.279	0.1723 ± 0.0028	7.0
FOX_23_10	cryoconite	429	78.1474	16.1136	10.8 ± 1.3	880 ± 32	0.210 ± 0.005	0.1612 ± 0.0083	7.7
FOX_23_11	cryoconite	430	78.1474	16.1138	13.3 ± 2.6	1240 ± 80	0.237 ± 0.014	0.1778 ± 0.0195	9.1
FOX_23_12	cryoconite	430	78.1474	16.1138	9.3 ± 3.4	930 ± 70	0.401 ± 0.022	0.1754 ± 0.0128	7.4
FOX 5.2.1.	bryophytes	NA	NA	NA	34.5 ± 4.8	1308 ± 85	1.725 ± 0.032	0.1718 ± 0.0040	68.9
FOX 5.2.4.	bryophytes	NA	NA	NA	23 ± 3	775 ± 44	0.387 ± 0.019	0.1804 ± 0.0132	81.2
FOX 5.2.5.	bryophytes	NA	NA	NA	20.6 ± 3.8	181 ± 30	0.061 ± 0.006	-	92.5
FOX 5.2.6.	bryoph	NA	NA	NA	<14	686 ±	0.303 ±	0.1577 ±	66.0

Polish Polar Research - Accepted Article

This article has been accepted for publication in a future issue of PPRes, but has not been fully edited. Content may change prior to final publication.

	ytes					59	0.023	0.0236	
FOX 5.2.7.	bryophytes	NA	NA	NA	31.9 ± 2.5	1592 ± 52	1.535 ± 0.063	0.1785 ± 0.0115	85.0
FOX 5.3.1. GM	glacier mice	424	78.1479	16.1129	30.6 ± 2	763 ± 26	0.618 ± 0.035	0.1780 ± 0.0169	29.5
FOX 5.3.2. GM (o.f.)	glacier mice	424	78.1479	16.1129	39.5 ± 4.9	1096 ± 70	0.504 ± 0.014	0.1793 ± 0.0119	26.1
FOX 5.3.2. GM (s.f.)	glacier mice	424	78.1479	16.1129	62.7 ± 3.6	1048 ± 37	0.946 ± 0.032	0.1730 ± 0.0136	6.6
FOX 5.3.3. GM	glacier mice	424	78.1479	16.1129	54 ± 2.3	1128 ± 35	1.084 ± 0.029	0.1701 ± 0.0058	17.8
FOX 5.3.4. GM	glacier mice	424	78.1479	16.1129	46 ± 1.9	1067 ± 33	1.227 ± 0.041	0.1175 ± 0.0049	19.6
FOX 5.3.5. GM	glacier mice	424	78.1479	16.1129	59.7 ± 2.8	890 ± 29	0.832 ± 0.027	0.1683 ± 0.0053	40.3
FOX 5.3.6. GM	glacier mice	424	78.1479	16.1129	25.7 ± 1.1	1181 ± 36	0.715 ± 0.027	0.1581 ± 0.0107	16.5
FOX 5.3.7. GM	glacier mice	424	78.1479	16.1129	30 ± 2	1043 ± 34	0.707 ± 0.028	0.1266 ± 0.0121	50.3
FOX 5.3.12. GM	glacier mice	424	78.1479	16.1129	27.1 ± 1.1	790 ± 24	1.166 ± 0.034	0.0834 ± 0.0054	10.3
FOX 5.3.13. GM	glacier mice	424	78.1479	16.1129	26.7 ± 1.5	1082 ± 35	0.805 ± 0.036	0.1261 ± 0.0082	22.6
FOX 5.3.14. GM	glacier mice	424	78.1479	16.1129	19 ± 0.8	1144 ± 35	0.473 ± 0.020	0.1579 ± 0.0091	15.3
FOX 5.3.16. GM	glacier mice	424	78.1479	16.1129	26.9 ± 1.7	614 ± 21	0.815 ± 0.026	0.1757 ± 0.0119	18.0
FOX 5.3.18. GM	glacier mice	424	78.1479	16.1129	27.8 ± 2	1495 ± 48	0.771 ± 0.022	0.1795 ± 0.0119	31.6
FOX 5.3.21. GM	glacier mice	424	78.1479	16.1129	32.3 ± 2.1	680 ± 24	0.905 ± 0.030	0.1882 ± 0.0100	27.2
FOX 5.3.23. GM (o.f.)	glacier mice	424	78.1479	16.1129	27.7 ± 5.7	1651 ± 133	0.389 ± 0.011	0.1804 ± 0.0098	63.3
FOX 5.3.23. GM (s.f.)	glacier mice	424	78.1479	16.1129	35.8 ± 3.8	1465 ± 53	0.677 ± 0.043	0.1538 ± 0.0185	8.2
FOX 5.3.24. GM	glacier mice	424	78.1479	16.1129	20.2 ± 1.4	964 ± 31	0.426 ± 0.018	0.1774 ± 0.0122	18.5
FOX 5.3.25. GM	glacier mice	424	78.1479	16.1129	27.4 ± 1.4	927 ± 29	0.782 ± 0.038	0.1795 ± 0.0132	23.2

Polish Polar Research - Accepted Article

Table S2. Quality control of gamma spectrometry. IAEA (International Atomic Energy Agency) activity concentrations of radionuclides in IAEA world-wide proficiency tests compared to those determined using a planar BEGe™ Canberra gamma counter at the Central Mining Institute – National Research Institute.

Radionuclide	IAEA activity concentration (Bq kg^{-1})	Measured activity concentration (Bq kg^{-1})
IAEA moss-soil material (IAEA-447)		

This article has been accepted for publication in a future issue of PPRes, but has not been fully edited. Content may change prior to final publication.

^{137}Cs	328 ± 8[a]	318 ± 19
^{210}Pb	311 ± 16[a]	308 ± 21
IAEA soil (IAEA-444)		
^{137}Cs	68.5 ± 1.4[b]	64.8 ± 5.9
^{210}Pb	48.0 ± 1.6[b]	59 ± 18

[a] IAEA (decay corrected to 2021)
[b] IAEA (decay corrected to 2007)

Table S3. Quality control results of the methods of mass spectrometry with IAEA certified standard.

Sample	Technique	Isotope	Certified value (Bq kg^{-1})	Measured value (Bq kg^{-1})
IAEA 447	mass spectrometry	^{240}Pu/^{239}Pu	0.186 ± 0.011[a]	0.186 ± 0.002
IAEA 447	mass spectrometry	$^{239+240}$Pu	5.3 ± 0.2[a]	5.27 ± 0.04

[a] Bu K., Cizdziel J.V. and Dasher D. 2013. Plutonium concentration and ^{240}Pu/^{239}Pu atomic ratio in biota collected from Amchitka Island, Alaska: recent measurements using ICP-SFMS. *Journal of Environmental Radioactivity* 124: 29–36, doi: 10.1016/j.jenvrad.2013.03.002.

Polish Polar Research - Accepted Article

This article has been accepted for publication in a future issue of PPRes, but has not been fully edited. Content may change prior to final publication.